Materials Research. 2024; 27:e20230378
DOI: https://doi.org/10.1590/1980-5373-MR-2023-0378

Effect of Acid Comonomer on the Morphology, Thermal, Mechanical and Solvent Stability Properties of Electrospun Membranes of Poly(Acrylonitrile-Co-Methacrylic Acid)

Luiz Guilherme Abreu de Paula[a*], Geilza Alves Porto[a], Ednildo Lopes de Alcântara Machado[b,c], Marcos Lopes Dias[a]

[a] *Universidade Federal do Rio de Janeiro, Instituto de Macromoléculas Professora Eloisa Mano, Av. Horácio Macedo, 2030, Cidade Universitária, 21941-598, Rio de Janeiro, RJ, Brasil.*
[b] *Universidade Federal Do Rio de Janeiro, Instituto de Biofísica Carlos Chagas Filho, Laboratório de Bioquímica de Insetos e Parasitos (Labip), 21941-902, Rio de Janeiro, RJ, Brasil.*
[c] *Instituto Nacional de Ciência e Tecnologia em Entomologia Molecular, Rio de Janeiro, RJ, Brasil.*

Received: August 25, 2023; Revised: November 29, 2023; Accepted: January 26, 2024

This study assessed the morphology and thermal, mechanical, and chemical properties of electrospun membranes made of acrylonitrile-methacrylic acid copolymers (PANCMAA). Copolymers were synthesized using the aqueous suspension method with varying comonomer contents (homopolymer,PAN, lower acid, PANCMAA1, and higher acid, PANCMAA2) and characterized by nuclear magnetic resonance (NMR) spectroscopy and gel permeation chromatography (GPC). Electrospun fibers were produced by adjusting the polymer concentration in the DMF solution, and the optimal conditions yielded nanofibrous membranes. PAN and PANCMAA membrane properties were evaluated by X-ray diffraction (XRD), differential scanning calorimetry (DSC), Dynamic Mechanical Thermal Analysis (DMTA), stress-strain tests, and swelling behavior in a phosphate buffer solution. The comonomer content influenced the crystallinity of the electrospun nanofibers, reducing the 16.8° XRD peak intensity from PAN to PANCMAA2. DSC indicated an increased T_g (from 113°C in PAN to 127°C in PANCMAA2) and a decreased exothermic cyclization enthalpy (311 $J.mg^{-1}$ in PAN to 271 $J.mg^{-1}$ in PANCMAA2). PANCMAA1 exhibited higher stiffness than PANCMAA2 and PAN, with a storage modulus of 0.16 GPa, a Young's modulus of 135.7 MPa, and a lower elongation at break (3.98%). The presence of the acid comonomer significantly enhanced the swelling behavior of the electrospun membranes in phosphate buffer solution.

Keywords: *Poly(acrylonitrile-methacrylic acid), copolymerization, thermo-mechanical properties, aqueous solvent resistance.*

1. Introduction

Electrospinning of nanofibrous membranes is a promising technology capable of creating nanostructures with high versatility of morphology and chemical compositions[1]. The intrinsic features of these membranes can allow a variety of applications, from biomedicine[2-4] to environmental bioremediation[5-7], with the main advantage of using a large variety of polymers to form different nanofibers and customized products with different porosities and interconnectivities[8].

Synthetic polymers such as poly(vinylidene fluoride) (PVDF), poly(ether-ether ketone) (PEEK), poly(ether sulfone) (PES), and acrylonitrile-based polymers (PAN) are known for their chemical stability in applications that require contact with aqueous media[9-12]. However, the production of nanofibers using PVDF, PES, and PEEK is more difficult because, in addition to the need of expensive solvents[13], these polymers are difficult to dissolve for the electrospinning process[14]. Acrylonitrile polymers are synthetic polymers with interesting properties (high stability in different solvents) for producing fibers, and are used by the industry to manufacture woven and non-woven mats and casting membranes[15].

The large surface area, volume ratio and small porosity size of electrospun nanofibers of acrylonitrile and the possibility of changing their wettability, allow to apply it in technologies of water and oil separation by adsorption processes, air filtration, removal of pathogenic agents and immobilizing organic molecules[7,15-19]. For example, incorporation of various fillers, including silver nanoparticles, TiO2, and metal-organic frameworks (MOFs) to PAN was used to fabricate non-woven mats characterized by high hydrophilicity, photocatalytic activity, and antibacterial properties. These mats demonstrate the capability to purify water by effectively removing oil, organic pollutants, and pathogens[20,21]. In this regard, presence of polar groups on the fiber surface either by using PAN copolymers containing polar comonomers or by surface chemical modification, play a pivotal role. These methods enable the anchoring of organic molecules with diverse functionalities or augmentation of adsorption capacity. Consequently, the non-woven mats acquire novel properties, transforming them into valuable tools for applications like biosensors or the removal of heavy metals[21-23]

*e-mail: luizguilhermeacm@ima.ufrj.br

The investigation of polyacrylonitrile nanofibers thermal properties is predominantly motivated by their promising application as precursors in the production of carbon fibers. Implemented strategies focus on regulating the cyclization reactions that occur within the side groups of PAN chains, leading to an enhancement in production yield[24]. Regarding mechanical characteristics, nanofibrous membranes, particularly those derived from polyacrylonitrile, exhibit a tendency towards lightweight and fragility, presenting handling challenges in the fabrication of membranes with applications like air filters[15]. In this context, the processing conditions for acrylonitrile-based polymers emphasize the minimization of fiber size[25]. Furthermore, the improvement of mechanical strength can be attained by blending with other polymers or production of composites with rigid fillers, along with the production of copolymers[15,25,26].

The properties of electrospun membranes of polyacrylonitrile can be tailored in different ways to change their crystallinity and mechanical and thermal properties[19,27,28]. When electrospun in blends with other polymers with different properties, such as polyethyleneimine (PEI) and poly(acrylic acid), membranes have been shown to become more hydrophilic and exhibit better mechanical strength[27,29]. Another way to improve fiber surface properties is to modify the chemical structure of PAN by copolymerization using comonomers that can also improve the thermal and physico-chemical properties depending on the purposes, like filtering process, for example[18,30].

The addition of methacrylic acid units to PAN molecules is an interesting option that could improve the molecular interaction and reactivity with organic molecules, thereby increasing its applicability. The presence of these carboxylic acid moieties increases the polarity of the PAN molecular chain (Figure 1). Consequently, the addition of acid groups in the structure of PAN increase its hydrophilicity and, depending on pH, increase its swelling capacity[31]

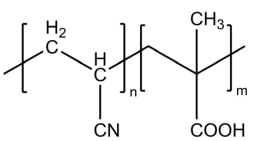

Figure 1. Chemical structure of poly (acrylonitrile-co-methacrylic acid).

For some biochemical applications, such as conjugation to proteins, it is important to consider the stability of the polymer in different buffers and pH conditions in coupling reactions. Electrospun membranes of PAN and their copolymers can be used to make these kinds of reactions, using a phosphate buffer solution as a solvent to succeed in reactions at neutral pH[32,33]. The main challenge is to obtain electrospun fibers of acrylonitrile copolymers containing high acid group content without lose properties, especially of surface morphology of nanofibers submitted to contact with aqueous solvent, avoiding the dissolution of nanofibers after the swelling effect during their contact with aqueous media at pH 7.

The objective of this research was to investigate the effects of aqueous buffered phosphate at pH 7.0 on the morphology of nanofibers made from acrylonitrile copolymers containing methacrylic acid, after swelling process. The motivation was the fact that most previous studies have focused on the effects of aqueous solvents on acrylonitrile nanofibers modified by fillers (composites), by crosslinking, or chemically modified by alkaline hydrolysis, and only the composites showed swelling behavior in buffered phosphate pH 7.0[34-36]. Additionally, the synthesis of acrylonitrile copolymers with methacrylic acid, the determination of electrospinning parameters (Figure 2), and the examination of their crystallinity, thermal, mechanical, and swelling properties will be addressed, discussing their potential applications.

2. Experimental

2.1. Materials

Acrylonitrile (99%) containing 35-45 ppm hydroquinone and methacrylic acid (99%) containing 250 ppm hydroquinone were purchased from Sigma-Aldrich. Both were purified by vacuum distillation to remove inhibitors. Potassium persulfate, ferrous ammonium sulfate (99%), and sodium metabisulfite (98%) were purchased from Sigma-Aldrich. Both were used without purification. Anhydrous ethanol and dimethylformamide were purchased from Sigma-Aldrich and used as received.

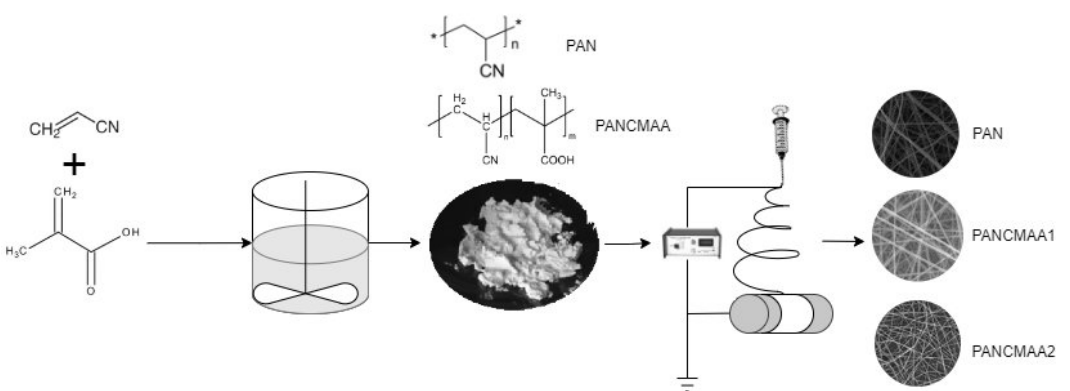

Figure 2. Schematic diagram of synthesis and design of acrylonitrile copolymer nanofibrous membranes.

2.2. Synthesis of acrylonitrile polymers

PAN and acrylonitrile-co-methacrylic acid copolymers (PANCMAA) were synthesized using deionized water suspension method at 50 °C under stirring and a nitrogen atmosphere, varying the methacrylic acid comonomer composition[37]. The molar fractions of the comonomers in the reaction feed were 7.5% (PANCMAA1) and 18.5% (PANCMAA2). Both PAN and PANCMAA copolymers were obtained after 3 h of reaction at 50 °C, by precipitating the white solid insoluble in water. The product was separated from water by filtration, rigorously washed with cold water and ethanol to remove residual monomers, and dried in a vacuum oven at 50 °C. The polymer was storage in room temperature for electrospinning processing.

2.3. Nanofibrous membranes

Electrospinning conditions of PAN and PANCMAA were tested using a Glassman high-voltage supply with 30 kV of capacity and a KD Scientific syringe pump 100-CE model, using an aluminum plate collector to recover the samples. PAN and PANCMAA were solubilized in dimethylformamide (DMF) at different concentrations for 12 h. Voltage of 20 kV, collector-needle distance of 20 cm and flow rates of 0.75 $ml.h^{-1}$ for PAN and 1.0 $ml.h^{-1}$ for PANCMAA1 and PANCMAA2, respectively, were used as spinning condition. The humidity and temperature were controlled to be 50-60% and 20°C, respectively.

An Electrospinning machine (E06 Nanofiberlabs, China) with two high voltage power suppliers with negative and positive output voltage capacity from 0 to ±30 kV, two syringe pump coupled and a roller collector with 200 mm wide and diameter of 80 mm with speed adjustable from 10 to 3000 rpm, was used to produce the nanofibrous membranes. The electrospinning set obtained previously was used to manufacture membranes by applying both negative and positive voltages in a ratio of 1:1, using the total voltage between 20 and 26 kV, and using a roller collector at the minimum speed (10 rpm) to avoid the orientation of the nanofibers. Membranes were obtained after 4 h of processing and dried in a vacuum oven at 60 °C to evaporate the residual solvent.

2.4. Characterization of polymers

The compositions of the PAN and PANCMAA copolymers were examined using Nuclear Magnetic Resonance (NMR) ^1H (Varian Mercury, VX-300, USA) operating at 300 MHz. Samples of 12 mg were dissolved in dimethyl sulfoxide-D_6 (0.6 mL) in 5 mm NMR tubes at 40 °C of temperature. The comonomer content was calculated by Equation 1, using the integers of the chemical shifts of CH_3 and CH_2 that are present in the comonomer methacrylic acid (MAA) and CH_2 of acrylonitrile monomer (AN) [25].

$$\%MAA = \left\{ 1 - \frac{I\left[CH_{2(AN)}(\beta) + CH_{2(MAA)}(\beta')\right] - I\left[\frac{2 * CH_{3(MAA)}}{3}\right]}{I\left[CH_{2(AN)}(\beta) + CH_{2(MAA)}(\beta')\right]} \right\} x100 \quad (1)$$

Where: β – the acrylonitrile monomer signal; β' – the methacrylic acid signal.

The molecular weights of the polymers were determined by Gel Permeation Chromatography (GPC) using a Shimadzu chromatograph (model UFLC, JAPAN). The chromatographer was equipped with a refractive index detector and a GPC-803 column (300 × 8.0 mm, Shimadzu). The analyses were performed at 30 °C using dimethyl formamide with 0.01 M LiBr[38] as the eluent at a flow rate of 1.0 $mL.min^{-1}$. Sample concentrations of 0.2% $m.v^{-1}$ and injection volumes of 20 µL were used. The number-average molecular weight (M_n), weight-average molecular weight (M_w), and dispersity index (Đ, M_w/M_n) were determined using a calibration curve with polystyrene standards (PS) in the range 700–2.2x10^6.

The morphology of electrospun membranes was examined by scanning electron microscopy (SEM) (MEV-FEG MIRA 4 LMU, TESCAN, USA), using a Denton Vacuum Desk II gold sputter to cover the nanofiber membranes. The average diameter of the electrospun fibers was measured from the SEM images using Image J software.

WAXD analyses were carried out in a Rigaku Miniflex diffractometer (Japan) using mats with dimensions of 2 × 2 cm. The analyses were performed using Cu Kα radiation (λ=1.5418 Å), with 2θ ranging from 5 °to 60° and a scanning speed of 0.05°/s.

The thermal properties were evaluated using differential scanning calorimetry (DSC) (Hitachi, High-Tech DSC7000 series, JAPAN). The samples were scanned on DSC 7 module of this thermal analyzer under nitrogen atmosphere at a flow rate of 50 $mL.min^{-1}$, and a heating rate of 10 $°C.min^{-1}$ from ambient temperature to 200°C. A sample weight of 4–6 mg in the form of a membrane was used to ensure good thermal contact. The samples were hermetically sealed.

The mechanical behavior of the electrospun membranes was examined using dynamic thermomechanical analysis (DMTA) (TA Instruments, Q800 series, USA) at an operating frequency of 1 Hz and a heating rate of 3 $°C.\ min^{-1}$. The samples were evaluated in the temperature range 25–200 °C. The tensile strength of the nanofibrous membranes was characterized using an Instron 5569 (USA) instrument with a load cell of 1 kN, crosshead speed of 2 $mm.min^{-1}$ and gauge length of 20 mm. Considering that the nanofibrous membranes are very thin and fragile, samples for the tensile mode test were mounted with aluminum foils at their ends in order to achieve a sufficiently strong grip[39]. All samples were rectangular with dimensions of 100 mm × 5 mm in accordance with the ASTM D882-10 standard test method.

The stability of the nanofibrous membranes was tested in a phosphate buffer aqueous solvent by immersing the membranes in 2 mL of 0.1 M phosphate buffer solvent. At intervals of 0, 5, 10, and 30 min and 1, 3, 6, 12, and 24 h, the samples were removed from the solution, dried with filter paper to remove excess liquid, and weighed. The objective was to determine the capacity of PAN and PANCMAA to absorb phosphate solution and to verify the possibility of dissolution of the membranes due to interaction with the solvent. Equation 2 was used to determine the retention of the solution in the nanofibers as a function of the immersion time.

$$\%swelling = \frac{W_t - W_0}{W_t} x100 \quad (2)$$

Where, W_t is the weight of membranes after the immersion and W_0 is the weight of membranes before the immersion.

3. Results and Discussion

3.1. Synthesis of PAN and PANCMAA

Figures 3a, 3b, and 3c show the ^{1}H NMR spectra of the polymers, and Figure 4 shows the logarithmic molecular weight distributions of the homopolymer (PAN) and copolymers of PANCMAA. As expected, the spectrum of PAN (Figure 3a) showed characteristic signals of CH and CH_2 at chemical shifts around 3.12 and 2.05 ppm, respectively. The spectra of PANCMAA1 (Figure 3b) and PANCMAA2 (Figure 3c) showed a signal at 1.24 ppm in addition to those signals, which are characteristic of CH_3 protons of methacrylic acid, with PAN and PANCMMA CH_2 signals superposed at 2.05 ppm[37]. Figure 4 shows that the copolymers had a broader molecular weight distribution than PAN.

Table 1 presents the comonomer content, polymerization yield, number-average molecular weight (M_n), weight-average molecular weight (M_w), and polydispersity (Đ) of PAN, PANCMAA1, and PANCMAA2. Calculation of the copolymer composition using Equation 1 showed that the methacrylic acid content incorporated in the acrylonitrile copolymer after the synthesis was 5.6% (PANCMAA1) and 8.7% (PANCMAA2), respectively. There was an increase in the molecular weight and dispersity of PANCMAA copolymers when compared with PAN. The best polymerization yield occurred for the preparation of PAN and PANCMAA1 because these polymers had low interactions with water and were easily filtered and recovered from the reaction medium. On the other hand, PANCMAA2 could not be easily separated from the water medium during the filtering step; therefore, it was necessary to separate the solid from the solution by rotary evaporation, and the dried solid product was powdered in a crusher mill, resulting in a lower yield.

3.2. PAN and PANCMAA nanofibrous membranes optimization

As described in the experimental section, the voltage, flow rate, needle tip-to-collector distance, and syringe needle used in the electrospinning process were previously determined by preliminary tests based on morphology visualization.

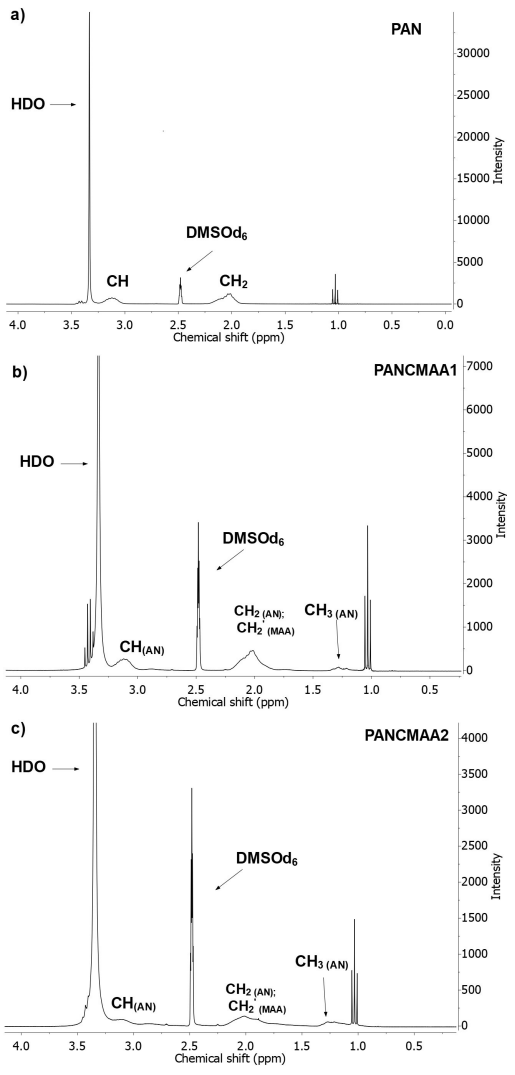

Figure 3. ^{1}H RMN spectra of (a) PAN, and (b) PANCMAA1 and (c) PANCMAA2 copolymers.

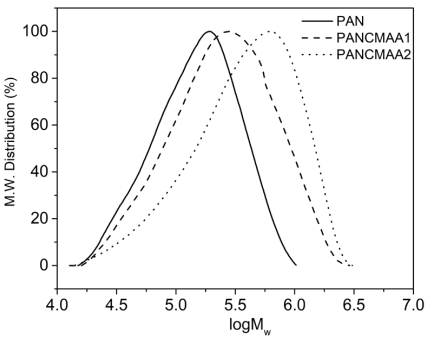

Figure 4. Molecular weight distribution of PAN, and PANCMAA1 and PANCMAA2 copolymers.

Table 1. Methacrylic acid content in feed and polymers, polymerization yield, average molecular weights (M_n and M_w) and dispersity index (Đ) of acrylonitrile polymers PAN, PANCMAA1 and PANCMAA2.

Sample	COOH Comonomer feed %	COOH comonomer in polymer %	Yield %	M_n	M_w	Đ
PAN	0	0	78	$1.06x10^5$	$2.08x10^5$	1.95
PANCMAA1	7.5	5.6	85	$1.50x10^5$	$3.83x10^5$	2.55
PANCMAA2	18.5	8.7	52	$2.22x10^5$	$5.68x10^5$	2.56

The choice of conditions was based mainly on discarding the areas where the beads were formed. Scanning Electron Microscopy (SEM) images and distribution of the average diameter of electrospun nanofibers as a function of PAN, PANCMAA1, and PANCMAA2 concentration in DMF are shown in Figures 5, 6, and 7, respectively. The average diameters of the nanofibers are listed in Table 2.

The differences in the polymer solution used for PAN, PANCMAA1, and PANCMAA2 are more closely related to the molecular weight of the samples (as shown in Table 1), which affects the viscosity of the solution and, consequently, the average diameter of the nanofibers and the possibility of defects, such as beads and broken fibers[40-43]. As a result, PAN required a higher concentration of polymer (15-20%) than PANCMAA1 (7.5-12.5%) and PANCMAA2 (5-10%).

In terms of morphology, the surface of the nanofibers in all three samples is relatively similar, with homogeneous nanofibers and some defects, such as beads (as shown in Figure 5a and 5b, Figure 6a and Figure 6b, and Figure 7b) and broken fibers (as shown in Figure 7a). These defects decreased with the increase in the concentration of the polymer solution in all samples. Therefore, we selected the following concentrations: 20.0 wt.vol^{-1}% for PAN (as shown in Figure 5c), 12.5 wt.vol^{-1}% for PANCMAA1 (as shown in Figure 6c), and 10.0 wt.vol^{-1}% for PANCMAA2 (as shown in Figure 7c). As shown in Table 2, PAN showed nanofibers with a diameter of 171 ± 38 nm, PANCMAA1 with a diameter of 213 ± 35 nm, and PANCMAA2 with a diameter of 258 ± 58 nm.

3.3. X-Ray Diffraction study

Wide Angle X-ray diffraction (WAXD) was used to observe possible structural and morphological changes in the nanofibers formed by the copolymers due to the addition of methacrylic comonomer. Figure 8 shows the WAXD curves of PAN, PANCMAA1, and PANCMAA2 nanofibrous membranes. The characteristic peak of paracrystalline PAN appeared in all samples at $2\theta = 16.8°$, which was attributed to the (1 0 0) plane of the PAN crystal lattice[29,44]. It was sharp in the PAN homopolymer and broader in the PANCMAA copolymers. A peak centered around $2\theta = 27°$, normally found in polyacrylonitrile powder[24,45], appears only in the PANCMAA1 copolymer and indicates second-order diffraction of the peak at 16.8°[29].

Table 2. Average diameter of nanofibers of PAN, PANCMAA1 e PANCMAA2 as function of polymer concentration in DMF.

Polymer	Concentration (wt.vol^{-1}%)	Average diameter (nm)
PAN	15.0	130 ± 48
	17.5	150 ± 35
	20.0	171 ± 38
PANCMAA1	7.5	165 ± 32
	10.0	188 ± 46
	12.5	213 ± 35
PANCMAA2	5.0	89 ± 21
	7.5	108 ± 36
	10.0	258 ± 58

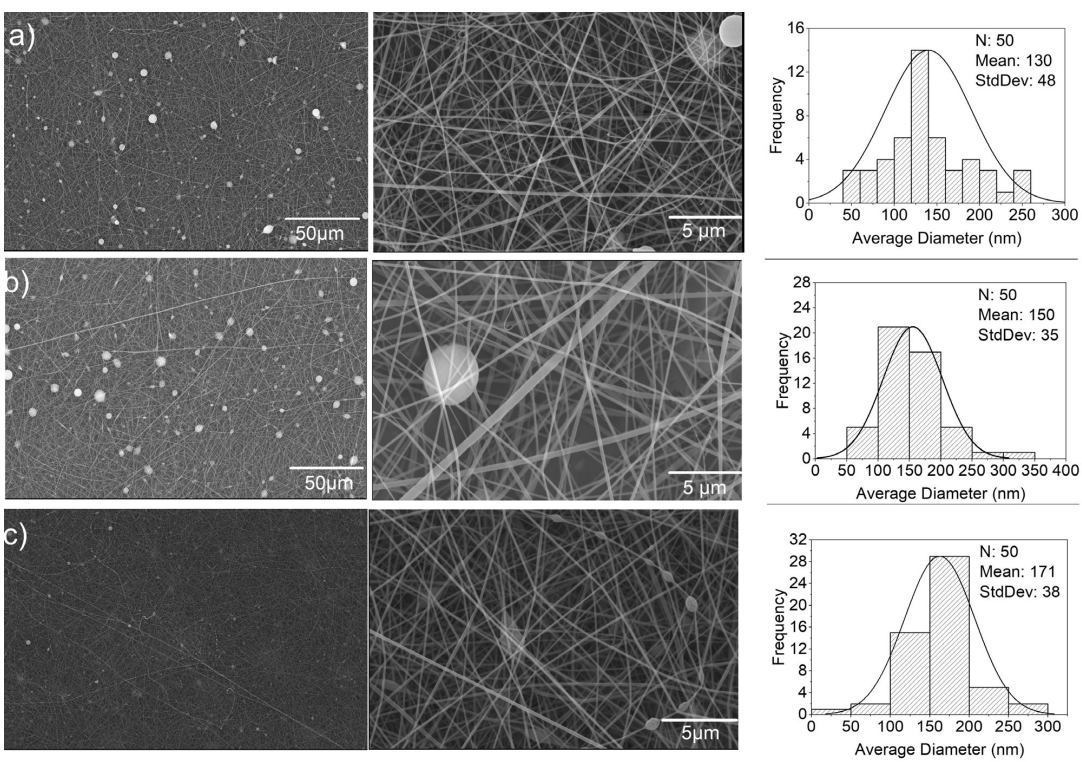

Figure 5. Morphology and diameter distributions of nanofibers in membranes of PAN as function of concentration in DMF: a) 15.0 wt.vol^{-1}, b) 17.5 wt.vol^{-1} and c) 20.0 wt.vol^{-1}.

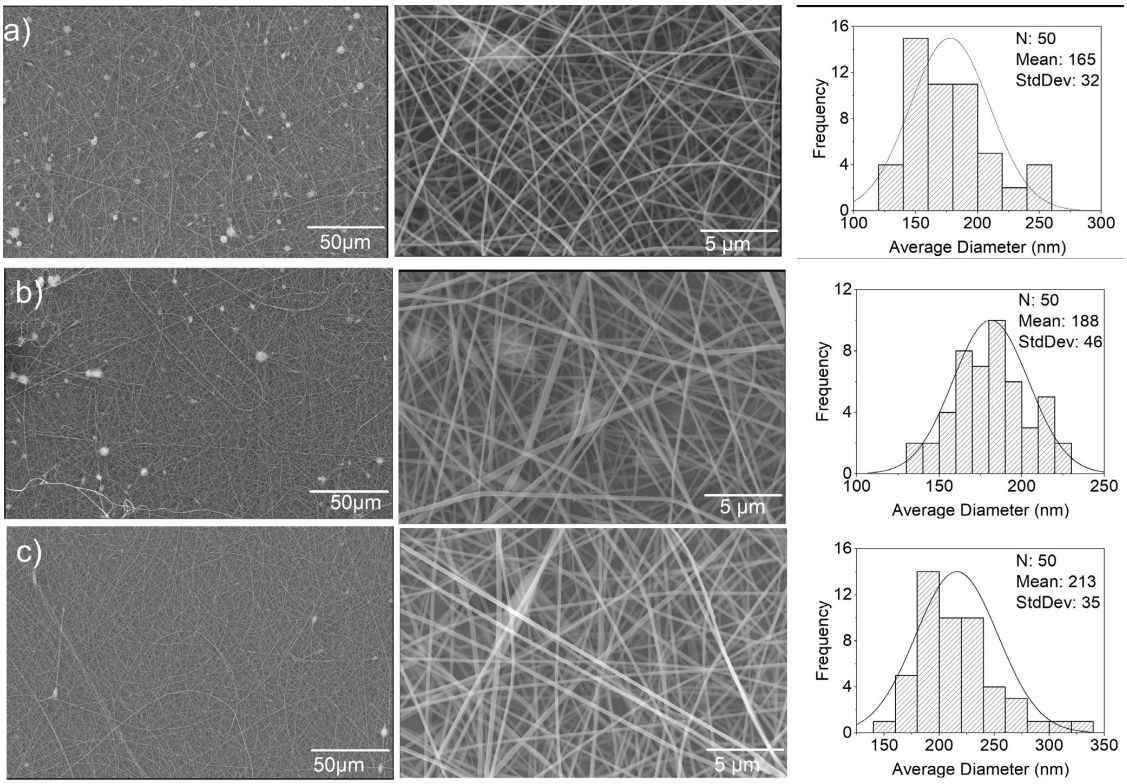

Figure 6. Morphology and diameter distributions of nanofibers in membranes of PANCMAA1 in function of concentration in DMF, in which: a) 7.5 wt.vol^{-1}; b) 10.0 wt.vol^{-1} and c) 12.5 wt.vol^{-1}%.

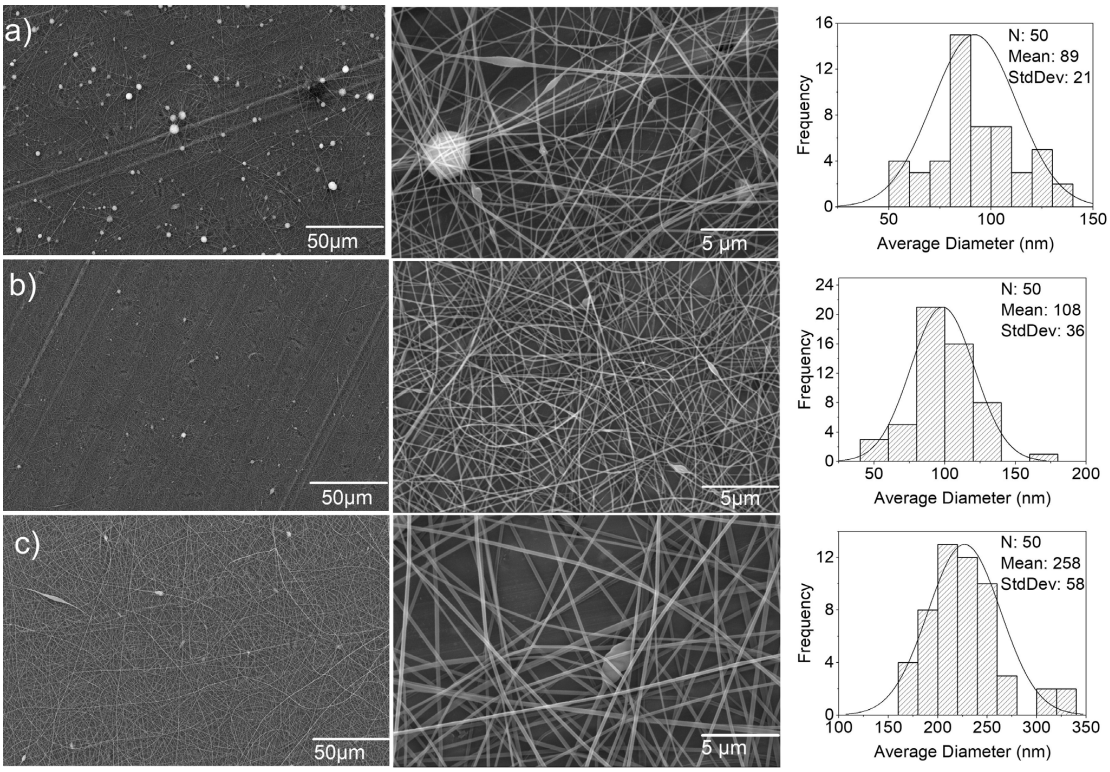

Figure 7. Morphology and diameter distributions of nanofibers in membranes of PANCMAA2 in function of concentration in DMF: a) 5.0 wt.vol^{-1}%; b) 7.5 wt.vol^{-1}% and c) 10.0 wt.vol^{-1}%.

The peak intensity (1 0 0 plane) of PANCMAA1 and PANCMAA2 decreases and becomes broader when compared by PAN homopolymer, indicating decreasing of degree of crystallinity due the existence of comonomer unities[46], in these case methacrylic acid.

3.4. Thermal Properties

The DSC curves of PAN, PANCMAA1, and PANCMAA2 are shown in Figure 9. The curves show the main events that occur with PAN-based polymers by heating, the glass transition, and the cyclization-dehydration reaction among nitrile groups at high temperatures. Table 3 summarizes the glass transition temperature (T_g) and typical cyclization information, such as onset (T_{onset}), maximum (T_{max}) and offset (T_{offset}) peak temperatures, and cyclization enthalpy (ΔH°) obtained from Figure 9.

In the region of PAN T_g, the copolymers present a smooth DSC curve profile. The T_g of electrospun acrylonitrile polymers shifted from 113 °C (PAN) to 127 °C (PANCMAA2). This occurs due to an increase in molecular interactions among the acid groups of the comonomers, which decreases the molecular relaxation[42].

At high temperatures (Figure 9), for all samples, the exothermic cyclization peak appears between 180 and 340 °C, presenting a sharp profile for PAN, whereas PANCMAA1 and PANCMAA2 present a broad peak profile. As shown in Table 3, the peaks of the electrospun PANCMAA copolymers began at lower temperatures (T_{onset}= 186 °C) and reached higher temperatures (329 °C and 336 °C) than those of electrospun PAN (from 228 °C to 322 °C), with PAN exhibiting a higher cyclization exothermic enthalpy (311 $J.mg^{-1}$). These peaks are associated with cyclization-dehydration reactions between the nitrile groups of polyacrylonitrile, initiated by free-radical mechanisms (CN groups of PAN) and radical and ionic mechanisms (COOH and CN groups in PANCMAA copolymers), and give rise to a cyclic ladder polymer structure from the linear molecular chain[29]. Furthermore, the addition of acid groups could influence the propagation of the cyclization reaction due to the intermolecular or intramolecular crosslinking of COOH and nitrile groups[47].

3.5. Mechanical Properties

The dynamic mechanical property curves of the nanofibrous membranes made of PAN, PANCMAA1, and PANCMAA2 are presented in Figure 10 (a: tan δ, b: loss modulus, and c: storage modulus). As shown in Figure 10a and 10b, the addition of an acid comonomer to PAN influences the viscoelastic behavior of the electrospun fibers. From the tan δ curves, we confirmed that the glass transition temperature (T_g) shifted to higher temperatures as the acid comonomer content increased. Considering that the tan δ peak of electrospun PAN contains two superposed peaks related to the molecular motion between ordered paracrystalline regions and amorphous regions with less order, the addition of comonomer acid altered the ordered regions, affecting the viscoelasticity of the electrospun fibers[48]. Consequently, this shifts T_g to higher values, corroborating the WAXD results shown in Figure 8, in which the peaks became larger with the addition of comonomer acids.

Figure 10c shows that the nanofibrous membranes exhibit a gradual increase in the storage modulus until the onset of T_g, being more pronounced in PAN nanofibers. This may have occurred due to a possible densification of the fiber mat of the samples[49,50]. The glass transition of PANCMAA1 and PANCMAA2 nanofibers exhibits an extended temperature range, as observed in both the loss modulus (Figure 10b) and storage modulus (Figure 10c).

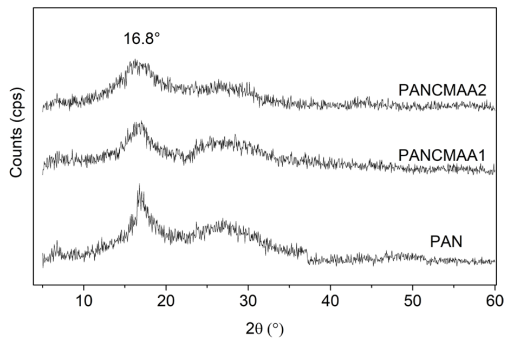

Figure 8. XRD pattern of PAN, and PANCMAA1 and PANCMAA2 copolymers.

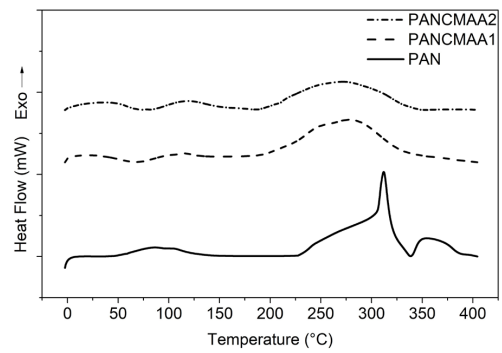

Figure 9. Thermogram behavior of PAN, and PANCMAA1 and PANCMAA2 copolymers.

Table 3. Values of glass transition temperatures (T_g), initial cyclization temperature (T_{onset}), maximum cyclization temperature (T_{max}), offset cyclization temperature (T_{offset}) and enthalphy of cyclization (ΔH°) of PAN, PANCMAA1 and PANCMAA2.

Sample	T_g (°C)	T_{onset} (°C)	T_{max} (°C)	T_{offset} (°C)	ΔH° ($J.mg^{-1}$)
PAN	113	228	312	322	311
PANCMAA1	120	186	278	329	278
PANCMAA2	127	186	270	336	271

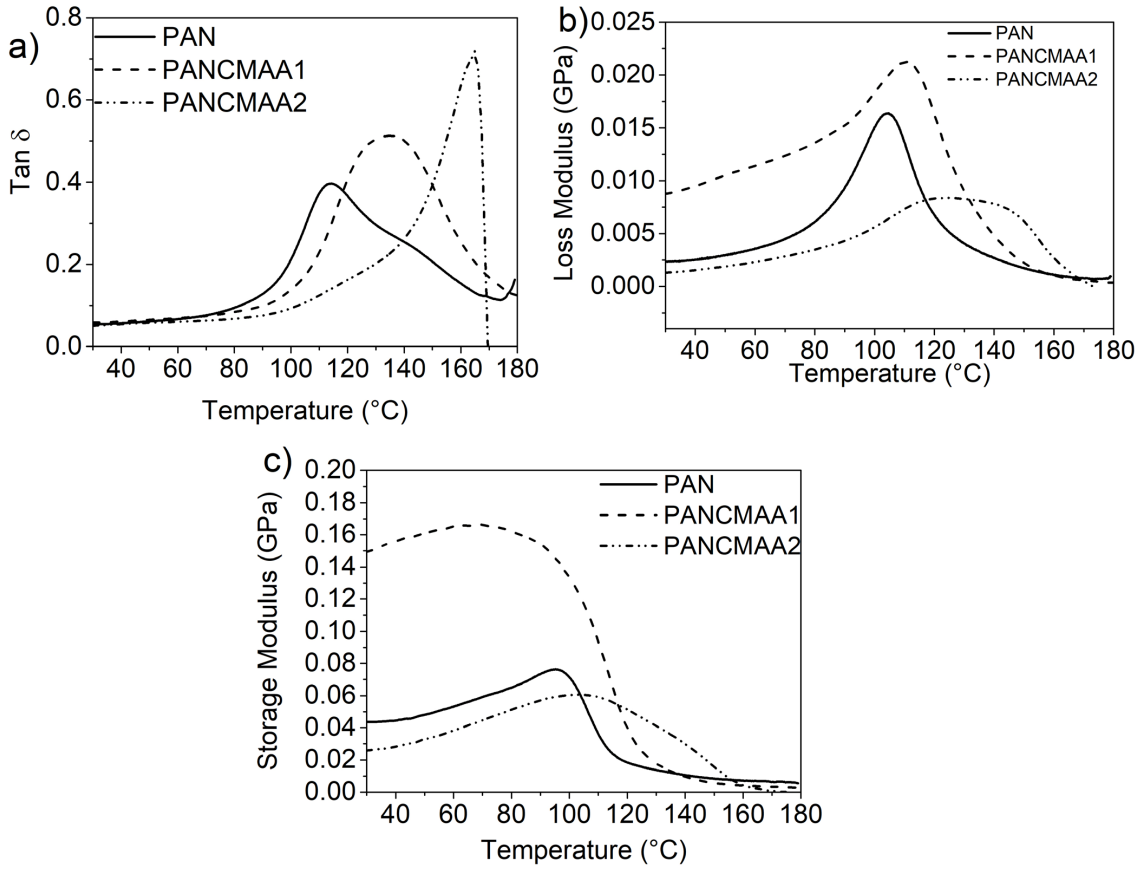

Figure 10. Dynamic mechanical analysis (DMTA) curves of the nanofibrous membranes of PAN, PANCMAA1 and PANCMAA2: a) Tan δ; b) Loss Modulus; and c) Storage Modulus.

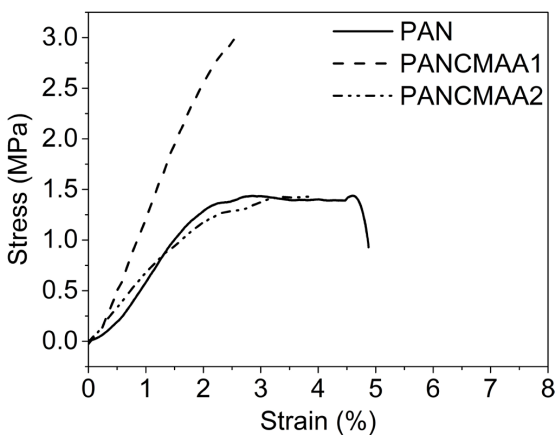

Figure 11. Stress-strain curves of PAN, PANCMAA1 and PANCMAA2 membranes.

This extended temperature range may be attributed to the incorporation of acid comonomers into the copolymers' molecular structure, which increased their amorphous phase and influenced their viscoelastic behavior. This effect is more pronounced in PANCMAA2 fibers than in PANCMAA1 fibers, which showed a slightly broadening of the loss modulus compared to the PAN homopolymer. It is worth noting that the stiffness of the fibers can be enhanced due to hydrogen bonding of the copolymers[51]. Consequently, the higher storage modulus values of PANCMAA1 fibers compared to PAN can be attributed to this phenomenon, as well as the lower amorphous phase when compared to PANCMAA2 copolymer.

Figure 11 shows the stress-strain curves of electrospun membranes made of PAN, PANCMAA1, and PANCMAA2, and Table 4 shows their quantitative data. It can be observed that the PANCMAA1 copolymer had different results when compared with PAN and PANCMAA2, that is, it had higher values of Young's modulus and ultimate strength and lower elongation at break. Gu et al.[52] found the same behavior in their work with addition of PVDF as nanofiller in PAN polymer solution to produce non-aligned electrospun nanofibers. Authors observed a decrease in breaking strength after PVDF concentration of 3%, suggesting that there is a limit of composition to improve the mechanical properties of PAN nanofibers. The high mechanical performance of PANCMAA1 can be explained by the good distribution of COOH commoners in the copolymer, which increases the dipolar interactions and, consequently, increases the stiffness of the nanofibers[27].

Table 4. Stress-strain curves of PAN, PANCMAA1 and PANCMAA2 membranes.

Sample	Young modulus (MPa)	Breaking strength (MPa)	Elongation at break (%)	Ref.
PAN/PVDF 0%	-	4	60	Gu et al.[52]
PAN/PVDF 1%	-	6	80	
PAN/PVDF 3%	-	8	55	
PAN/PVDF 5%	-	4	60	
Twisted PAN nanofibers	391.3	34.9	4.1	Yan et al.[26]
oPAN210	52.3±4.6	1690±148	28±3	Zou et al.[53]
coPAN	3100-12400	304-595	24-189	Xu et al.[25]
PAN	91.7 ± 12.6	1.53 ± 0.17	3.98 ± 0.43	This work
PANCMAA1	135.7 ± 12.7	2.62 ± 0.28	2.87 ± 0.6	This work
PANCMAA2	77.12 ± 5.6	1.41 ± 0.12	4.19 0.18	This work

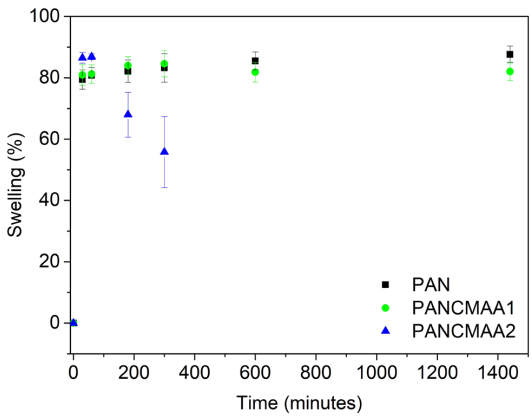

Figure 12. Swelling behavior of PAN, PANCMAA1 and PANCMAA2 membranes.

Table 4 suggests that the mechanical properties of the samples are lower than those reported in the literature. The electrospun polyacrylonitrile (PAN) samples were modified chemically or physically to enhance their properties for specific applications. These modifications include adding PVDF as nanofillers in PAN nanofibers for waterproof and breathable applications[52], pre-oxidizing PAN homopolymer[53], aligning fibers using a drawing process in PAN copolymer nanofibers[25], or by twisting[26].

3.6. Swelling Behavior

Figure 12 shows the swelling behavior of PAN, PANCMAA1, and PANCMAA2 electrospun membranes in phosphate buffer (pH 7.4), which is commonly used to react with proteins. It can be observed that all the membranes retained 80–90% of water in approximately 30 min. PAN and PANCMAA1 showed higher stability over time, maintaining their weight stability even 24 h after immersion in phosphate buffer solution. After 3 h of immersion in phosphate buffer, PANCMAA2 showed a decrease in the weight of the fibers that were effectively weighed according to the methodology. It was impossible to measure the weight after 5 h (300 min). It is known that polymers based on acrylic acids are sensitive to aqueous media because of the formation of strong hydrogen bonds between the acid groups of the polymer, water, and ionic bonds with salt ions, causing swelling of the nanofiber mats[31,54]. The use of acrylonitrile-methacrylic acid copolymers with acid content of 8.5% to produce electrospun membranes and the high surface area of the membrane increased the interaction of these copolymers with the phosphate buffer, decreasing the stability of the nanofibers in this medium.

Considering the results of the swelling assay, the morphologies of the electrospun membranes of PAN, PANCMAA1, and PANCMAA2 before and after immersion in a 0.1 M phosphate buffer solution (pH 7.4) were evaluated using scanning electron microscopy (SEM) (Figure 13). The diameter of the PAN and PANCMAA1 nanofibers increased after immersion in phosphate buffer, which was more evident in PANCMAA1 (Figure 13d). An increase in the surface porosity was also observed. The ionic interaction between the phosphate salts and the COOH groups of methacrylic acid in the copolymers could increase the affinity between the aqueous solvent and the electrospun nanofibers, causing swelling and, consequently, modifying the morphology of the nanofiber surface[54]. With the increase in methacrylic acid groups in the copolymer PANCMAA2, the high affinity between electrospun nanofibers and the aqueous solvent affected its morphology, with disaggregation of the nanofibers during the immersion time (Figure 13f).

Therefore, PANCMAA1 could be the best choice in conditions where phosphate buffered solutions are used, such as biomolecule immobilization[32,55]. In this case, reactive groups such as COOH are necessary to react with the reactive terminal groups of the biomolecule under controlled neutral pH conditions, without losing the nanofiber morphology during the reaction process. Other possibilities can be their application for environmental treatment and bioremediation processes, both for water purification through water and oil separation, making it possible to produce superhydrophobic nanofibrous membranes with high cleaning capacity[20], removal of fluorides, heavy metals, and organic and inorganic pollutants through molecular affinity adsorption[18,56,57], and filtration of particles present in the air. These applications are related to molecular affinity adsorption processes and electrostatic attractions, enhanced by the large surface area of the nanofibers and the chemical nature of the copolymers[19,22,58].

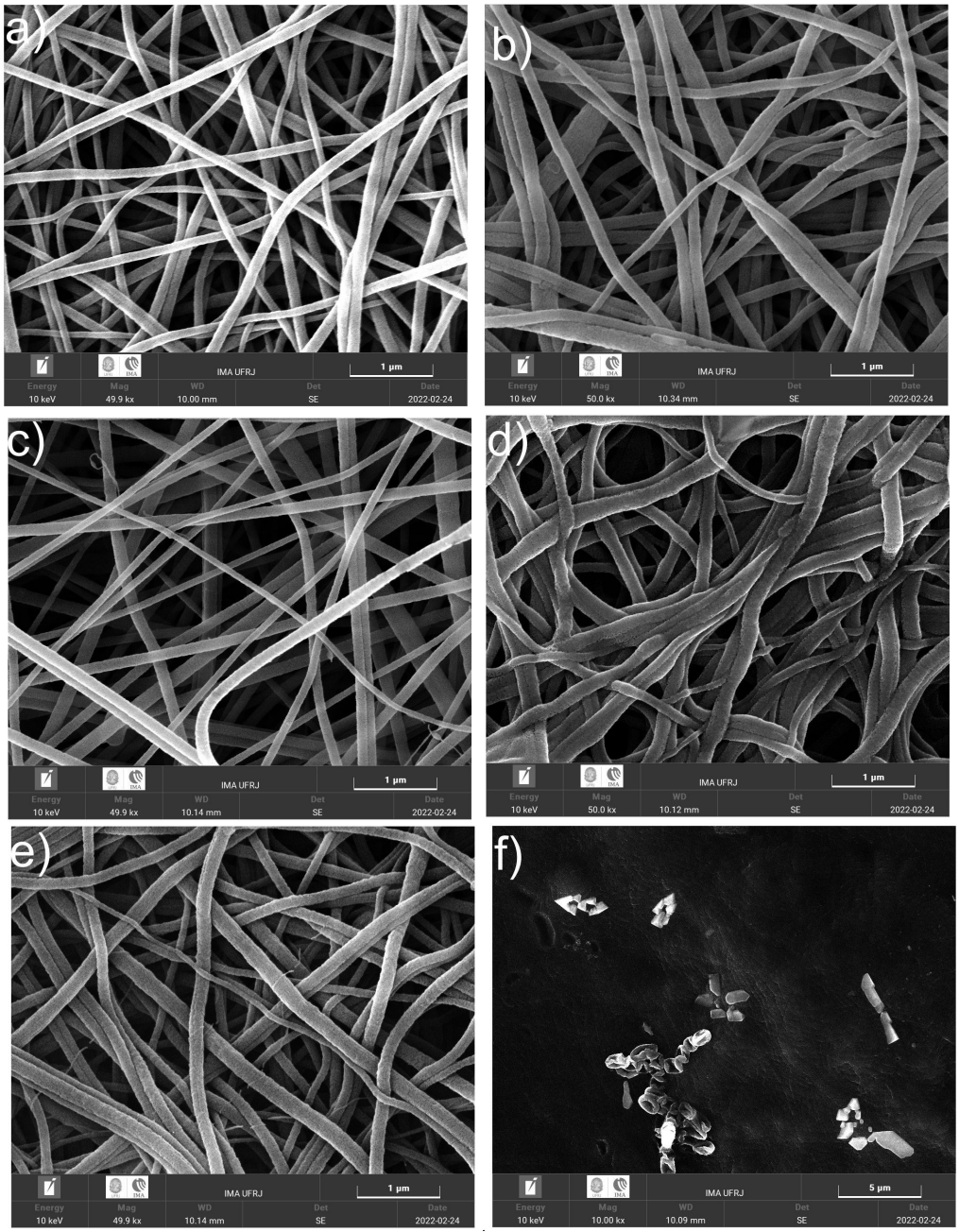

Figure 13. SEM images of electrospun membranes of PAN, PANCMAA1 and PANCMAA2 before (a, c, e) and after swelling test (b, d, f), respectively. Scale of 1 µm (Figures 13a-e) e 5 µm (Figure 13f).

4. Conclusions

This study showed that the content of acid groups in polyacrylonitrile copolymers directly affects the morphology and thermal properties of nanofibrous membranes, as observed by DSC, XRD, and swelling assays. This behavior was not evident when considering the mechanical properties, as observed from the DMTA and tensile tests. From a thermal point of view, considering the DSC and DMTA studies, glass transition (T_g) and thermal cyclization events are directly affected by the presence and content of acid groups in these polymers, affecting the viscoelastic behavior of the membranes. The influence of the acid monomer was observed mainly in the mechanical dynamic analysis and in the PAN cyclization reaction at high temperatures, as indicated by DSC. As observed from the X-ray diffraction data, these electrospun PAN-based nanofibers became more amorphous as the content of the acid comonomer increased in the copolymer, which was intensified by the electrospinning process owing to fast chain stretching and solvent evaporation and solidification, which hindered possible polymer crystallization.

In terms of the mechanical properties, there was no clear behavioral relationship between the presence of acid co-units in the copolymer and the stiffness of the nanofibrous membranes. Membranes prepared with the lower content of acid copolymer shows higher stiffness than those made with PAN and the higher acid content copolymer. The results of both the storage modulus from DMTA and Young's modulus from tensile tests demonstrate that there is a certain limit of acid comonomer content for an increase in membrane stiffness, making it more mechanically resistant.

Regarding the swelling of these electrospun membranes, an increase in the acid group content in the copolymer increased the affinity of the nanofiber surface with the aqueous phosphate-buffered solvent, affecting the dimensional stability. Consequently, fiber disintegration occurs after a certain contact time of immersion in membranes made with copolymer with high acid comonomer content. Because of this behavior, the percentage of acid comonomers in the copolymer must be considered in applications that involve the use of buffer solutions containing phosphate, mainly those related to biochemical reactions of proteins with PAN-based polymers, in which neutral pH control is fundamental.

5. Acknowledgments

Authors thank the Coordenação de Aperfeiçoamento de Pessoal de Nível Superior (CAPES), Conselho Nacional de Desenvolvimento Científico e Tecnológico (CNPq) (Grant 307364/2018-6), FAPERJ (Grants E-26/202.538/2019 and SEI-260003/000311/2023) and Project nº 022019 Nanotechnology Research Networks Program in the State of Rio de Janeiro (grant E-26/010.000979/2019) for financial support.

6. References

1. Sirelkhatim N, Parveen A, LaJeunesse D, Yu D, Zhang L. Polyacrylonitrile nanofibrous mat from electrospinning: born with potential anti-fungal functionality. Eur Polym J. 2019;119:176-80.
2. Leal M, Leiva Á, Villalobos V, Palma V, Carrillo D, Edwards N et al. Blends based on amino acid functionalized poly (ethylene-alt-maleic anhydride) polyelectrolytes and PEO for nanofiber elaboration: biocompatible and angiogenic polyelectrolytes. Eur Polym J. 2022;173:111269.
3. Pedrosa MCG, dos Anjos SA, Mavropoulos E, Bernardo PL, Granjeiro JM, Rossi AM et al. Structure and biological compatibility of polycaprolactone/zinc-hydroxyapatite electrospun nanofibers for tissue regeneration. J Bioact Compat Polym. 2021;36(4):314-33.
4. Toledo ALMM, Ramalho BS, Picciani PHS, Baptista LS, Martinez AMB, Dias ML. Effect of three different amines on the surface properties of electrospun polycaprolactone mats. Int J Polym Mater Polym Biomater. 2021;70(17):1258-70.
5. Kharaghani D, Khan MQ, Tamada Y, Ogasawara H, Inoue Y, Saito Y et al. Fabrication of electrospun antibacterial PVA/Cs nanofibers loaded with CuNPs and AgNPs by an in-situ method. Polym Test. 2018;72:315-21.
6. Kim SJ, Park WH. Polydopamine- and polyDOPA-coated electrospun poly(vinyl alcohol) nanofibrous membranes for cationic dye removal. Polym Test. 2020;89:106627.
7. Guo W, Guo R, Pei H, Wang B, Liu N, Mo Z. Electrospinning PAN/PEI/MWCNT-COOH nanocomposite fiber membrane with excellent oil-in-water separation and heavy metal ion adsorption capacity. Colloids Surf A Physicochem Eng Asp. 2022;641:128557.
8. Bellan LM, Craighead HG. Applications of controlled electrospinning systems. Polym Adv Technol. 2011;22(3):304-9.
9. Fashandi H, Yegane A, Abolhasani MM. Interplay of liquid-liquid and solid-liquid phase separation mechanisms in porosity and polymorphism evolution within poly(vinylidene fluoride) nanofibers. Fibers Polym. 2015;16(2):326-44.
10. Sun F, Ren HT, Huang SY, Li TT, Peng HK, Lin Q et al. Polyvinylidene fluoride electrospun fibers loaded TiO2 for photocatalytic degradation and oil/water separation. Fibers Polym. 2020;21(7):1475-87.
11. Porto GA, de Paula LGA, Arias JJR, Chaves EG, Marques MFV. Comparative analysis of poly(ether-ether-ketone) properties aged in different conditions for application in pipelines. J Therm Anal Calorim. 2023;148(1):79-95.
12. Li X, Teng S, Xu X, Wang H, Dong F, Zhuang X et al. Solution blowing of polyacrylonitrile nanofiber mats containing fluoropolymer for protective applications. Fibers Polym. 2018;19(4):775-81.
13. Daraeinejad Z, Shabani I. Enhancing cellular infiltration on fluffy polyaniline-based electrospun nanofibers. Front Bioeng Biotechnol. 2021;9:641371.
14. Ekambaram R, Dharmalingam S. Fabrication and evaluation of electrospun biomimetic sulphonated PEEK nanofibrous scaffold for human skin cell proliferation and wound regeneration potential. Mater Sci Eng C. 2020;115:111150.
15. Selvam AK, Nallathambi G. Polyacrylonitrile/silver nanoparticle electrospun nanocomposite matrix for bacterial filtration. Fibers Polym. 2015;16(6):1327-35.
16. Mohammad N, Atassi Y. Adsorption of methylene blue onto electrospun nanofibrous membranes of polylactic acid and polyacrylonitrile coated with chloride doped polyaniline. Sci Rep. 2020;10(1):13412.
17. Liu Y, Park M, Ding B, Kim J, El-Newehy M, Al-Deyab SS et al. Facile electrospun Polyacrylonitrile/poly(acrylic acid) nanofibrous membranes for high efficiency particulate air filtration. Fibers Polym. 2015;16(3):629-33.
18. Barbosa B, Santos MR, Oliveira HP. Electrospun fibers of copolymers for the removal of ionic dyes: the influence of processing variables. Fibers Polym. 2018;19(1):94-104.
19. Bansal P, Purwar R. Development of efficient antimicrobial zinc oxide modified montmorillonite incorporated polyacrylonitrile nanofibers for particulate matter filtration. Fibers Polym. 2021;22(10):2726-37.
20. Lu T, Liang H, Cao W, Deng Y, Qu Q, Ma W et al. Blow-spun nanofibrous composite self-cleaning membrane for enhanced purification of oily wastewater. J Colloid Interface Sci. 2022;608:2860-9.
21. Lu T, Deng Y, Cui J, Cao W, Qu Q, Wang Y et al. Multifunctional applications of blow-spinning setaria viridis structured fibrous membranes in water purification. ACS Appl Mater Interfaces. 2021;13(19):22874-83.
22. Rajabi S, Shaki H. Efficient removal of lead and copper from aqueous solutions by using modified polyacrylonitrile nanofiber membranes. Fibers Polym. 2021;22(3):694-702.
23. Jiang D, Zheng M, Ma X, Zhang Y, Jiang S, Li J et al. Rhodamine-anchored polyacrylamide hydrogel for fluorescent naked-eye sensing of Fe3+. Molecules. 2023;28(18):6572.
24. Qiao MM, Kong HJ, Ding XM, Hu ZF, Yu MH. Study on the crystallization behavior of PAN fibers during hot-drawing process in supercritical carbon dioxide fluid with different strain. In: Materials Science Forum. Proceedings. Switzerland: Trans Tech Publications Ltd; 2020. vol. 976, p. 84-9
25. Xu TC, Han DH, Zhu YM, Duan GG, Liu KM, Hou HQ. High strength electrospun single copolyacrylonitrile (copan) nanofibers with improved molecular orientation by drawing. Chin J Polym Sci. 2021;39(2):174-80.
26. Yan T, Tian L, Pan Z. Structures and mechanical properties of plied and twisted polyacrylonitrile nanofiber yarns fabricated by a multi-needle electrospinning device. Fibers Polym. 2016;17(10):1627-33.

27. Bigogno RG, Dias ML, Manhães MBN, Sanchez Rodriguez RJ. Integrated treatment of mining dam wastewater with quaternized chitosan and PAN/HPMC/AgNo3 nanostructured hydrophylic membranes. J Polym Environ. 2022;30(4):1228-43.
28. Khan S, Zulfiqar X, Khan T, Khan R, Khan M, Khattak SA, et al. Investigation of structural, optical, electrochemical and dielectric properties of SnO2/GO nanocomposite. J Mater Sci Mater Electron. 2019;30:10202.
29. Liu H, Zhang S, Yang J, Ji M, Yu J, Wang M et al. Preparation, stabilization and carbonization of a novel polyacrylonitrile-based carbon fiber precursor. Polymers (Basel). 2019;11(7):1150.
30. Dhakate SR, Gupta A, Chaudhari A, Tawale J, Mathur RB. Morphology and thermal properties of PAN copolymer based electrospun nanofibers. Synth Met. 2011;161(5-6):411-9.
31. Huang J, Huang ZM, Bao YZ, Weng ZX. Temperature and pH response, and swelling behavior of porous acrylonitrile-acrylic acid copolymer hydrogels. Chin J Polym Sci. 2006;24(2):195-203.
32. Aghababaie M, Beheshti M, Bordbar AK, Razmjoua A. Novel approaches to immobilize Candida rugosa lipase on nanocomposite membranes prepared by covalent attachment of magnetic nanoparticles on poly acrylonitrile membrane. RSC Advances. 2018;8(9):4561-70.
33. Xu R, Chi C, Li F, Zhang B. Laccase–polyacrylonitrile nanofibrous membrane: highly immobilized, stable, reusable, and efficacious for 2,4,6-trichlorophenol removal. ACS Appl Mater Interfaces. 2013;5(23):12554-60.
34. Haider MK, Sun L, Ullah A, Ullah S, Suzuki Y, Park S, et al. Polyacrylonitrile/Carbon Black nanoparticle/Nano-Hydroxyapatite (PAN/nCB/HA) composite nanofibrous matrix as a potential biomaterial scaffold for bone regenerative applications. Mater Today Commun. 2021;27:102259.
35. Haider MK, Ullah A, Sarwar MN, Yamaguchi T, Wang Q, Ullah S et al. Fabricating antibacterial and antioxidant electrospun hydrophilic polyacrylonitrile nanofibers loaded with AgNPs by lignin-induced in-situ method. Polymers (Basel). 2021;13(5):748.
36. Liu H, Lo Hsieh Y. Preparation of water-absorbing polyacrylonitrile nanofibrous membrane. Macromol Rapid Commun. 2006;27(2):142-5.
37. Bajaj P, Paliwal DK, Gupta AK. Acrylonitrile–acrylic acids copolymers. I. Synthesis and characterization. J Appl Polym Sci. 1993;49(5):823-33.
38. Azuma C, Dias ML, Mano EB. Molecular weight determination of acrylonitrile polymers by gel permeation chromatography in N,N-dimethylformamide. Makromol Chemie Macromol Symp. 1986;2(1):169-78.
39. Robert B, Nallathambi G. Highly oriented poly (m-phenylene isophthalamide)/polyacrylonitrile based coaxial nanofibers integrated with electrospun polyacrylonitrile-silver nanoparticle: application in air filtration of particulate and microbial contaminants. J Appl Polym Sci. 2022;139(23):52294.
40. Anaya Mancipe JM, Lopes Dias M, Moreira Thiré RMDS. Type I collagen – poly(vinyl alcohol) electrospun nanofibers: FTIR study of the collagen helical structure preservation. Polym Technol Mater. 2022;61(8):846-60.
41. Rodrigues BVM, Cabral TS, Sgobbi LF, Delezuk JAM, Pessoa RS, Triboni ER et al. A simple and green method for the production of nanostructured materials from poly(vinyl alcohol)/graphene quantum dots. Mater Chem Phys. 2018;219(August):242-50.
42. Almafie MR, Marlina L, Riyanto R, Jauhari J, Nawawi Z, Sriyanti I. Dielectric properties and flexibility of polyacrylonitrile/graphene oxide composite nanofibers. ACS Omega. 2022;7(37):33087-96.
43. Hossain N, Silva R, Goh KL, Pasbakhsh P. Unidirectionally aligned and randomly oriented electrospun nanofibrous polyacrylonitrile membranes. In: Dong Y, Baji A, Ramakrishna S, editors. Electrospun polymers and composites. United Kingdom: Elsevier; 2021. p. 361–81. Woodhead Publishing Series in Composites Science and Engineering.
44. Fu Z, Liu B, Deng Y, Ma J, Cao C, Wang J et al. The suitable itaconic acid content in polyacrylonitrile copolymers used for PAN-based carbon fibers. J Appl Polym Sci. 2016;133(38)
45. Ryšánek P, Benada O, Tokarský J, Syrový M, Čapková P, Pavlík J. Specific structure, morphology, and properties of polyacrylonitrile (PAN) membranes prepared by needleless electrospinning; Forming hollow fibers. Mater Sci Eng C. 2019;105:110151.
46. Zhang G, Chen L, Qiu L, Xu X, Feng J. Preparation and characterization of poly (Acrylonitrile-co-1-Acryloylpyrrolidine-2-Carboxylic Acid) with high molecular weight. J Macromol Sci Part B. 2013;52(9):1298-308.
47. Lei S, Wu S, Gao A, Cao W, Li C, Xu L. The formation of conjugated structure and its transformation to pseudo-graphite structure during thermal treatment of polyacrylonitrile. High Perform Polym. 2017;29(9):1097-109.
48. Barua B, Saha MC. Studies of reaction mechanisms during stabilization of electrospun polyacrylonitrile carbon nanofibers. Polym Eng Sci. 2018;58(8):1315-21.
49. Zhong T, Liu W, Liu H. Green electrospinning of chitin propionate to manufacture nanofiber mats. Carbohydr Polym. 2021;273(June):118593.
50. Cho M, Karaaslan M, Chowdhury S, Ko F, Renneckar S. Skipping oxidative thermal stabilization for lignin-based carbon nanofibers. ACS Sustain Chem& Eng. 2018;6(5):6434-44.
51. Gumrukcu S, Soprunyuk V, Sarac B, Yüce E, Eckert J, Sarac AS. Electrospun polyacrylonitrile/2-(acryloyloxy)ethyl ferrocenecarboxylate polymer blend nanofibers. Mol Syst Des Eng. 2021;6(6):476-92.
52. Gu J, Quan Z, Wang L, Zhang H, Wang N, Qin X et al. Fiber-microsphere binary structured composite fibrous membranes for waterproof and breathable applications. Fibers Polym. 2022;23(6):1500-9.
53. Zou Y, Jiang S, Hu X, Xu W, Chen Z, Liu K, et al. Influence of pre-oxidation on mechanical properties of single electrospun polyacrylonitrile nanofiber. Mater Today Commun. 2021;26:102069.
54. Abdulhamid MA, Muzamil K. Recent progress on electrospun nanofibrous polymer membranes for water and air purification: A review. Chemosphere. 2023;310:136886.
55. Ye P, Xu ZK, Wu J, Innocent C, Seta P. Nanofibrous Membranes Containing Reactive Groups: electrospinning from Poly(acrylonitrile- c o -maleic acid) for Lipase Immobilization. Macromolecules. 2006;39(3):1041-5.
56. Cui J, Li F, Wang Y, Zhang Q, Ma W, Huang C. Electrospun nanofiber membranes for wastewater treatment applications. Separ Purif Tech. 2020;250(April):117116.
57. Jian S, Cheng Y, Ma X, Guo H, Hu J, Zhang K et al. Excellent fluoride removal performance by electrospun La–Mn bimetal oxide nanofibers. New J Chem. 2022;46(2):490-7.
58. Deng Y, Lu T, Cui J, Keshari Samal S, Xiong R, Huang C. Bio-based electrospun nanofiber as building blocks for a novel eco-friendly air filtration membrane: a review. Separ Purif Tech. 2021;277(August):119623.